Fuel Cell Behavior and Energy Balance on Board a Hyundai Nexo

Jules Sery, Pierre Leduc

Fuel cell behavior and energy balance on board a Hyundai Nexo

Jules Sery and Pierre Leduc

Abstract

Hydrogen fuel consumption measuring methodologies of a fuel cell vehicle without modifying the fuel path has been tested and benchmarked. In this work, they are applied to a Hyundai Nexo fuel cell electric vehicle driving different mission profiles on a chassis dynamometer. Three methods respectively based on hydrogen tank pressure, tailpipe oxygen concentration, and IR-shared (infrared) tank data are compared to the reference method relying on fuel cell current measurements. In addition to the hydrogen fuel consumption results, the installed electrical measuring equipment made possible to yield the fuel cell efficiency map at both stack and system levels as well as the energy consumption of its balance-of-plant (BoP) components during steady-state operation. A maximum steady-state efficiency of 66.8% is reported along with a rated system power of 82 kWe involving a 9.1-kWe power consumption for the electric compressor. It is shown that the compressor and the 12-V accessories are the most energy consuming devices among the BoP components accounting for 2%–3% of the total electric energy generated by the fuel cell. Furthermore, the behavior of the powertrain system is monitored and discussed during warm-up phases and during a long idling period. Finally, based on non-intrusive temperature measurements, a short analysis is conducted about the temperature impact on the fuel cell efficiency.

Keywords

Fuel cell vehicle testing, hydrogen consumption measurement methods, fuel cell system energy balance

Introduction

Associated to a low-carbon electricity generation, electric vehicles account for one of the major ways toward a decarbonized transport for the future.[1,2] As far as road transport is concerned, two types of electric vehicles can be considered: pure battery or with a hydrogen fuel cell. The later technology is generally seen as offering higher range and faster refueling/recharge and, for trucks, to an increased freight capacity. On the other hand, its total value chain energy efficiency is dramatically less: with the same amount of grid electricity, a battery electric vehicle (BEV) will drive at least 2 to 3 times longer trips than the equivalent fuel cell electric vehicle (FCEV)[3–5] This is due to the energy consumption needed to produce and transport the hydrogen before it can be used to refill a vehicle and also to a lower powertrain efficiency. Then, from a tank-to-wheel perspective, it is of paramount importance to analyze the energy consumption of FCEVs and how the electricity is used on board, in order to continue the optimization of this part of the value chain.

Hydrogen Fuel Cell Electric Vehicles can be seen as parallel hybrid vehicles with the engine being replaced by a fuel cell. In the Hyundai Nexo the 95-kW fuel cell stack takes the role of the prime mover whereas the 1.56 kWh Li-ion battery purpose consists in helping the fuel cell during transient loads as well as during low loads. More importantly it unlocks regenerative braking opportunities.[6,7] The fuel cell system consists of a stack operating with other components (air compressor, humidifier, cooling system, etc.) called BoP (Balance of Plant) when considered as a whole.[8] It is of interest to investigate the power consumption of each component to draw an exhaustive energy balance of the vehicle powertrain on various mission profiles.

To supply the fuel cell with hydrogen, three high pressure tanks are located under-floor at trunk level. This hydrogen storage system is capable of holding 6.33 kg of compressed gas at 70 MPa under nominal

IFP Energies nouvelles, Institut Carnot IFPEN Transports Energie, Rueil-Malmaison, France

Corresponding author:
Jules Sery, Transportation Department, IFP Energies nouvelles, Institut Carnot IFPEN Transports Energie, 1 et 4 avenue de Bois-Préau, Rueil-Malmaison 92852, France.
Email: jules.sery@ifpen.fr

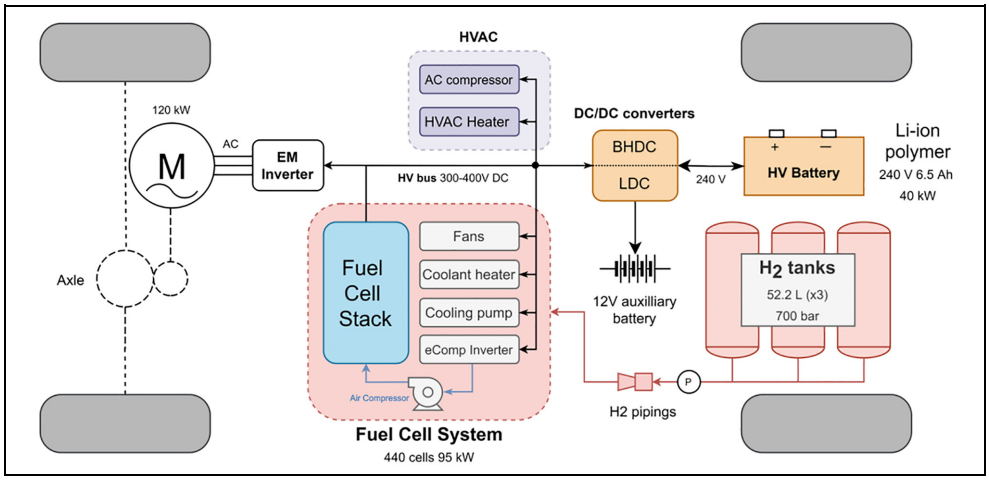

Figure 1. Powertrain diagram of the Hyundai Nexo.

conditions. The vehicle powertrain architecture is illustrated in Figure 1.

Hydrogen-powered vehicle testing necessarily involves the use of a specific method to measure the fuel consumption. WLTP standard advocates for employing the gravimetric method which requires using external hydrogen storage tanks.[9] Those tanks are weighted before and after the test to determine the average fuel consumption over the test. Alternatively, manufacturers can opt for two different methods provided that they can prove them to be sufficiently accurate. Those two methods are respectively the pressure method and the flow method. Along with the gravimetric one they are the recommended normative methods in ISO 23828 and SAE J2572 standards.[10,11] Pressure method is based on the measurement of both tank pressure and temperature. Assuming that the tank volume is known, the fuel consumption can be easily derived. The flow method requires measuring the hydrogen flow by using a dedicated sensor placed somewhere inside the fuel path (e.g. a Coriolis mass flow sensor as recommended in SAE J2572). Except for the pressure one all of the last cited methods require very intrusive instrumentation or the use of external specific device. Another method, investigated in this paper, consists in measuring the oxygen concentration at exhaust to determine hydrogen consumption.[12]

In this paper a method based on the fuel cell current measurement has been set up to be used as a reference. In parallel the pressure method has been tested thanks to the signal derived from the hydrogen tank pressure sensor. In order to improve accuracy a tank model is used to calculate hydrogen gas temperature evolution throughout the driving cycle to correct the hydrogen mass derived from the hydrogen equation of state (EoS). Furthermore, a module, dedicated to communication with the hydrogen tanks through the infrared emitter located at fueling nozzle level, was developed for this work. The tank pressure and temperature could be then monitored but only with vehicle "ignition" off.

Various driving cycles have been run on a chassis dynamometer with a dedicated instrumentation of the fuel cell system to investigate the performances and the fuel consumption of the vehicle on a variety of use cases including a long idling period.

The literature on fuel cell vehicle chassis dynamometer testing is far from abounding. In 2018 Argonne U.S. DOE laboratory exhaustively tested a Toyota Mirai on a roller test bench.[13,14] An on-road evaluation of several FCEVs was performed by NREL[15] but with anonymized and normalized data. Green NCAP[16] tested a Hyundai Nexo over different driving cycles and published associated fuel consumption results. Yet no details regarding fuel cell system efficiency values and energy balance were reported.

Chassis dynamometer test campaign

Vehicle instrumentation

Electrical currents have been measured in the electric powertrain for the following components:

- Fuel cell stack (LEM® HTR 500-SB sensor).
- e-Compressor invertor.
- Low voltage DC/DC converter (LDC) output.
- High voltage DC/DC converter (BHDC) output.
- Cooling pump.
- Coolant heaters.
- Fans.
- Li-ion polymer battery output.

The different clamp-type current sensors have been connected to an electrical Power Analyzer Hioki® PW3390 (except for the fuel cell stack). All the BoP components are supplied with the voltage produced by the fuel cell. Thus, measuring the fuel cell stack voltage as well as electrical currents listed above is sufficient to draw quite-complete component-wise energy balances. It is noteworthy to point out that the communication

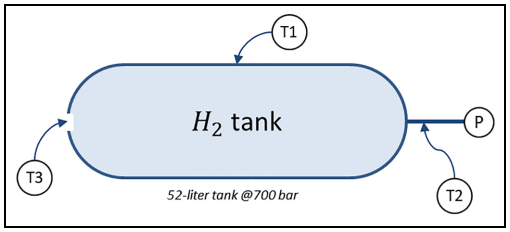

Figure 2. H_2 storage tank instrumentation.

Table 1. Test campaign summary.

Cycle	Type	Start
WLTC (× 3 types)	10°C, 23°C, FBS,	Cold
R_WLTC	Reversed cycle	Cold
RDE	Compliant	Cold
FTP75	Urban	Hot/cold averaged
US06	Dynamic	Hot
HWFET	Highway	Hot
JC08	Urban	Hot/cold averaged
BAB130	Highway	Hot
FC cycle (Figure 3)	Power sweeps	Hot

FBS: full battery start. Hot/cold averaged: fuel consumption results are averaged between the cold start and the hot start cycles.

with vehicle through its OBD-II interface could not be achieved during this testing campaign.

Besides the electrical instrumentation that was carried out on the electric powertrain, the hydrogen pressure was collected from the original vehicle sensor by reverse-engineering of its transfer function. The temperature was measured at three levels (Figure 2):

- Tank envelope (T_1).
- Tank inlet/outlet pipe (T_2).
- Tank bottom nozzle, a metallic part in contact with the gas (T_3).

To monitor vehicle warm-up three temperatures were measured at fuel cell system level using type T thermocouples:

- Fuel cell housing surface (T_{fc}).
- Cooling pump housing (T_{cp}).
- Radiator fins (T_{rad}).

Measuring actual coolant temperature at stack level would have been too much intrusive with respect to study security constraints. Yet, T_{cp} turned out to be the closest to fuel cell expected temperature ~80°C.

All the study measurements were recorded at 10 Hz.

Tests carried out on chassis dynamometer

The study involved various driving cycles in order to investigate the vehicle performances on multiple use types such as typical driving conditions, urban, and dynamic driving, highway driving and fuel cell efficiency mapping cycle. The following driving cycles were tested twice to achieve repeatability on a chassis dyno (where not specified temperature is 23°C) (Table 1):

The vehicle road-load parameters and mass were taken as being equal to the settings employed for the approval WLTC cycle (Table 2).

Table 2. Vehicle mass and road-load parameters used in the test campaign.

Vehicle mass	2057 kg
Road-load	
a	178.7 N
b	0.919 N/(km/h)
c	0.04037 N/(km/h)^2

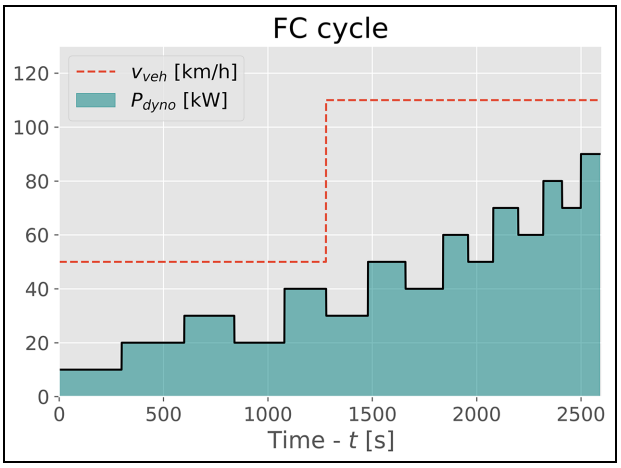

Figure 3. Fuel cell system power sweep cycle. The step in vehicle speed is meant to alleviate fuel cell heat load duty on high power points. Constant load measurements are carried out on increasing and decreasing wheel power levels.

Fuel consumption measurement methods

The reference method: Fuel cell current-based

Each electron produced by the fuel cell basically comes from the consumption of a proton H^+ at the catalytic layer level of the membrane electrode assembly (MEA). One can derive a direct relationship between the current flowing through one cell of the stack and the corresponding amount of hydrogen mass flow. Knowing the cells number, it yields the hydrogen mass flow rate:

$$\dot{m}_{H_2} = \frac{I_{stack} N_{cell} M_{H_2}}{nF} \quad (1)$$

With M_{H_2} [g/mol] the hydrogen molar mass, n the number of mole of electron per mole of H_2 consumed, F [C/mol] the Faraday constant, I_{stack} [A] the stack current and N_{cell} the number of cells (=440).

Inconvenience of this method lies in the fact that it cannot account for any possible hydrogen purge operated at anode side. Likewise, any hydrogen leakage through the fuel cell membrane cannot be quantified using this method.

Yet, without considering hydrogen purges impact on fuel flow, this method constitutes a good reference and a robust way of evaluating instantaneous hydrogen flow and consequently of reporting fuel consumption. Indeed, system operation is usually done suchlike the anode pressure is always above cathode one so that to mitigate nitrogen and water vapor permeation through the membrane. This generally reduces the need to purge the anode.[17]

The pressure method

Taking advantage of pressure measurements, the hydrogen mass trapped in the tanks can be instantaneously derived using the gas EoS. Even though the internal temperature cannot be recorded, an approximation based on a thermodynamic model of the hydrogen tank is calculated. Assuming that the hydrogen temperature is uniform inside the tank and invoking the hydrogen EoS, one can apply the conservation of energy to the tank:

$$m_{H_2} c_v \frac{\mathrm{d}T}{\mathrm{d}t} = \dot{m}_{H_2}(c_p - c_v)T + GS_{tank}(T_1 - T) \quad (2)$$

$$PV_{tank} = Zm_{H_2} rT \quad (3)$$

With T [°K] being the equivalent hydrogen temperature in tank, m_{H_2} [kg] the hydrogen mass trapped into the tank, V_{tank} [m^3] the volume, P [Pa] the tank pressure, Z [-] the compressibility factor, c_p and c_v [J/°K/kg], respectively the constant pressure and volume heat capacities and GS_{tank} [W/°K] the global heat exchange coefficient. Thermodynamic properties (c_p, c_v, Z) are determined using CoolProp,[18] a C++ library (a Python wrapper was used) offering calculation capabilities of physical properties for various fluids including hydrogen. The model is implemented and solved using the Python SciPy library ODE solver featuring an explicit Runge–Kutta numerical integration method. To determine the global heat exchange coefficient GS_{tank} a sequenced tank recharge has been carried out in a hydrogen station. The same model as described above, but considering $\dot{m}_{H_2}$ as being equal to zero, has been fitted to the pressure measurements during tank resting periods (Figure 4).

Values ranged from 50 to 80 W/°K. Uncertainties in these results originate from the different hydrogen flow regimes that are encountered inside the tank. Therefore, depending on the regime, the heat exchanged by natural convection occurring at internal wall level will vary in intensity. Similarly this coefficient is subject to variation depending on the mass flow rate at which hydrogen exits or enters the tank. For the sake of simplification it is considered that GS_{tank} is a constant equal to 70 W/°K.

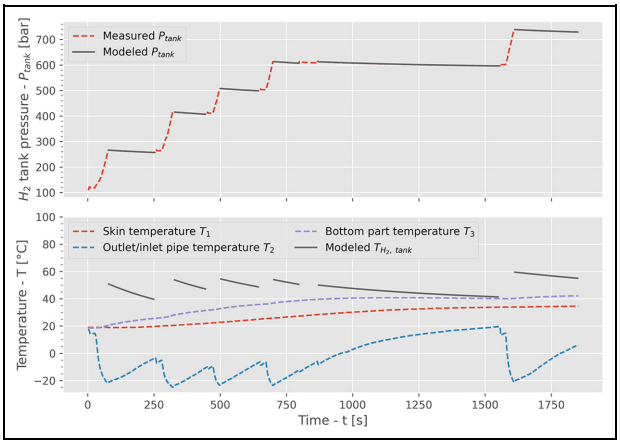

Figure 4. Closed tank model fitted to pressure measurements during tank resting phases of a sequenced hydrogen recharge. At each stop, the station operator had access to the tank temperature communicated by the vehicle.

For all the tests run on the roller test bench both current and pressure methods were used to compare their results in terms of fuel consumption.

The IR–PT method

In order to optimize the hydrogen tanks fueling strategy the FCEVs are usually equipped with an IR emitter at fueling nozzle level. This emitter provides the fueling station with some data related to the tank type as well as further physical measurements such that tank pressure, temperature, and volume. The communication protocol follows the SAE J2799 standard.[19] This protocol has been implemented within an infrared IR module specifically developed for this study. Nevertheless the vehicle was found to communicate only with the ignition turned off. Consequently, measurements were made just before and after a test to determine the difference in hydrogen pressure and temperature. Using the hydrogen EoS and knowing the tank volume it is then possible to calculate a normative fuel consumption that complies with the SAE J2572 standard pressure method. Yet, even though results are expected to be close to the pressure method ones, they could deviate depending on the tank temperature sensor location (this location could not be identified in the vehicle).

The O_2 method

Oxygen concentration was measured at exhaust level using an oxygen analyzer (magneto-pneumatic detection type). Exhaust gas flow was measured using a Pitot tube at vehicle tailpipe along with pressure and temperature. All the flow outlets upstream the measuring equipment were blocked to ensure that the measure yields the actual flow rate. Knowing the fuel cell oxygen

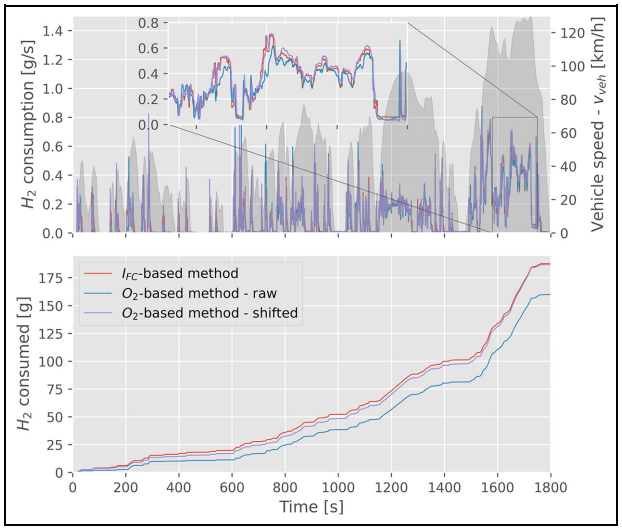

Figure 5. Comparison of fuel cell-current based method and time-shifted O_2 method on a WLTC.

consumption it is possible to determine the hydrogen one. Yet, this method suffers from the same inconvenience as the fuel cell current-based method in that it cannot account for hydrogen purges and leakages. Indeed, the oxygen consumption is a direct image of the part of consumed hydrogen which participated to the electron creation (equation (5)). Oxygen consumption is determined following equation (4):

$$\dot{m}_{O_2} = \rho_{O_2}(20^oC,\ 1\ atm)Q_{air}\left(X_{O_2,lab} - X_{O_2,tp,s}\right) \quad (4)$$

$$\dot{m}_{H_2} = 2\frac{M_{H_2}}{M_{O_2}}\dot{m}_{O_2} \quad (5)$$

With Q_{air} [Nm^3/s] being the measured flow rate at normal conditions for temperature and pressure (20°C, 1 atm), $X_{O_2,lab}$ [-] the oxygen concentration in the laboratory, $X_{O_2,tp,s}$ [-] the time-shifted oxygen concentration at tailpipe and M_{O_2} [g/mol] the oxygen molar mass.

The calculated oxygen mass flow rate has to be shifted in time[12] knowing the measured flow rate and the exhaust pipes total volume V_p [m^3] upstream the gas analyzer. Indeed the pipes volume induces a time lag τ [s] between the oxygen consumed at fuel cell level and the one measured at tailpipe level. This time lag is such that the following equation (6) is verified:

$$V_p = \int_t^{t+\tau} Q_{air}(t)dt \quad (6)$$

$$X_{O_2,tp,s}(t) = X_{O_2,tp}(t + \tau(t)) \quad (7)$$

The exhaust pipes total volume was approximated based on pipes diameter and length at $V_p = 16L$.

Hydrogen consumption measuring methods comparison

Figure 5 compares the evolution of hydrogen consumption determined with both fuel cell current-based method and O_2-method on a WLTC. When correcting the raw O_2-method with the time shift related to gas time transit inside exhaust pipes the two methods end up yielding very close results.

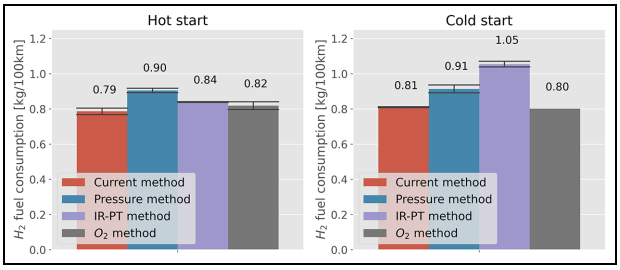

Figure 6. Comparison of the fuel consumption measurement methods on WLTC cycle for both hot and cold start conditions.

Figure 6 shows fuel consumption results yielded using the four above-described methods on WLTC cycles. Both IR-PT and pressure methods give higher hydrogen consumption as compared to fuel cell current-based method and O_2-method. Differences are very likely to lie in the fact that hydrogen purges are accounted for in IR-PT and pressure methods. Discrepancies between IR-PT and pressure methods might be explained by the temperature which is considered to determine the hydrogen mass trapped in tanks. Indeed pressure method relies on an estimated hydrogen tank temperature (see related section) whereas IR-PT method involves a temperature measurement at tank level.

Fuel cell system efficiency measurements

During the FC cycle the vehicle was subject to a sequence of increasing constant loads. The measurements were averaged over a time window upon which the fuel cell and all BoP components reached steady-state operation. Furthermore time windows sizes were adapted so that the HV battery was no longer found to supply any current. Fuel cell efficiency at stack level and at system level is defined as follows:

$$\eta_{stack} = \frac{V_{stack}I_{stack}}{\dot{m}_{H_2}LHV} \quad (8)$$

$$\eta_{FCS} = \frac{P_{stack} - P_{BoP}}{\dot{m}_{H_2}LHV} \quad (9)$$

With V_{stack} [V] being the stack voltage, P_{stack} [kW] the fuel cell stack power and LHV [J/kg] the hydrogen higher heating value. The BoP power consumption is calculated leveraging equation (10).

$$P_{BoP} = P_{eComp} + P_{heater} + P_{fans} + P_{c,pump} \quad (10)$$

With P_{eComp} [kW] being the eCompressor power at inverter level, P_{heaer} the fuel cell stack coolant heater power, P_{fans} the fans DC motors power and $P_{c,pump}$ the coolant pump power. The stack voltage was measured installing an electrical contact at the direct output

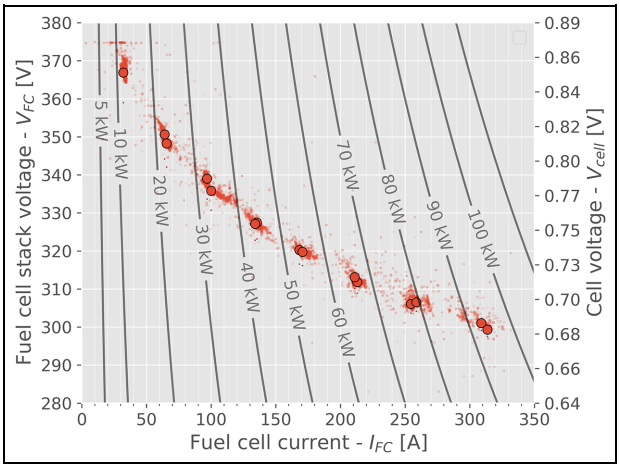

Figure 7. Fuel cell steady-state polarization curve measurements. Scattered shaded points in the background are 10 Hz data on averaging time windows. Iso-power lines denote stack power.

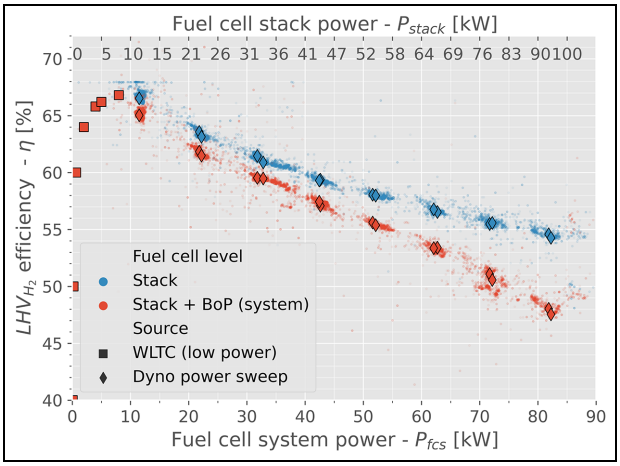

Figure 8. Fuel cell system and stack efficiency values on steady-state operation.

of the fuel cell. The reference current method was used to determine the hydrogen consumption $\dot{m}_{H_2}$ (Figures 7–9).

At maximum wheel power reached on steady-state operation of the dynamometer, a fuel cell power of 82 kWe was measured at system level and 94 kWe at stack level. The corresponding efficiencies were respectively equal to 48% and 54.4% with respect to hydrogen LHV. The maximum fuel cell efficiency is found to be 66.8% at system level and 67.5% at stack level. This maximum efficiency is located at 8–10 kWe system power which roughly translates to 10% of maximum system power. Additionally, the electric air compressor consumed up to 9.1 kWe (Figure 13). The electric coolant pump was responsible for 600 We of BoP power consumption on maximum power point. Below 50 kWe its contribution was negligible (< 200 We). Above 40 kWe power the fans motors consumption started to

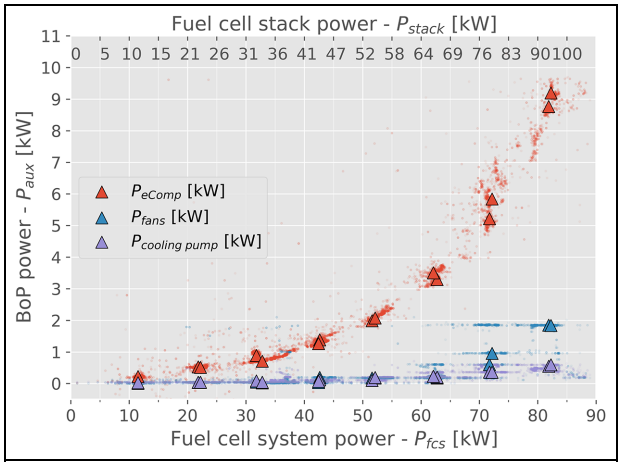

Figure 9. BoP components power consumption on steady-state operation. Coolant heater was never found to be operated on these points.

significantly increase: starting from 200 We and soaring up to 1.8 kWe on maximum load points.

Fuel consumption measurements

Comparison of pressure and current methods

This work was split in two different testing campaigns separated by a four-month period. The IR module only worked for WLTC cycles in Figure 6 corresponding to the second testing campaign. Thus for the other tests the initial tank temperature was considered to be equal to T_3. Figure 12 compares the evolution of hydrogen mass in tank for three model settings: isothermal (constant hydrogen temperature no matter what), adiabatic (no heat exchange with environment) and with heat exchange ($GS_{tank} = 70$ W/°K). These first 2 incomplete model settings respectively overestimate and underestimate hydrogen mass consumed throughout the cycle. Accounting for heat exchange turns out to yield the closest results to the reference fuel cell current-based method. Regarding temperature measurements T_3 revealed to be the closest to hydrogen temperature with a decreasing tendency. Conversely, T_1 and T_2 measurements revealed to be increasing, regardless of hydrogen temperature evolution, as a consequence of the heat flowing under floor rejected by the coolant radiator.

Influence of battery SOC cycle variation on hydrogen consumption

In order not to introduce an error in the hydrogen fuel consumption evaluation, the energy balance has to be corrected by the battery SOC variation throughout the test. Hydrogen raw consumption FC_{rawH_2} is then corrected using equation equation (11).

$$FC_{H_2} = FC_{rawH_2} + K_{H_2} EC \tag{11}$$

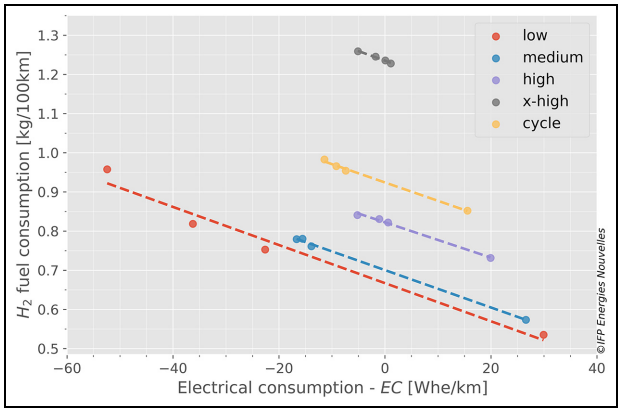

Figure 10. Fuel consumption as a function of electrical energy consumption at battery level. Only WLTC cycles @23°C are represented. Positive EC means energy has been consumed at the battery.

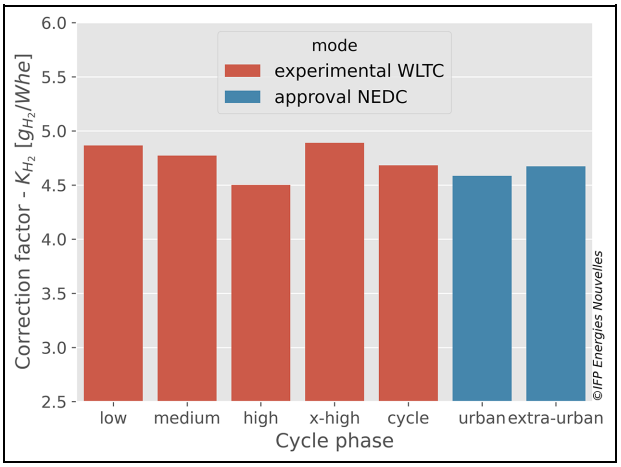

Figure 11. Calculated correction factors for WLTC as compared with the ones used in the approval NEDC tests.

$$EC = \frac{\int V_{batt} I_{batt}}{d_{cycle}} \tag{12}$$

With FC_{H_2} [kg/100 km] being the corrected hydrogen consumption, K_{H_2} [kg/Whe] the correction factor, EC [Whe/km] the electrical energy consumption, V_{batt} [V] and I_{batt} [A] respectively the battery potential and the battery current and d_{cycle} [km] the driving cycle distance.

K_{H_2} is determined by calculating the slope of linear fitting curves on Figure 10 for each phase of the WLTC cycle. In this paper when dealing with a cycle involving mostly urban behavior the coefficient fitted on low WLTC phases is employed. Similarly the extra-high WLTC phase is used to correct consumption for highway cycles (i.e. HWFET and BAB130). For RDE cycles the WLTC cycle correction factor is used.

Figure 11 illustrates the comparison between the fuel consumption correction factors determined experimentally on WLTC and the ones considered in the approval NEDC test.

Results

Hydrogen consumption over typical driving cycles. Globally the FCEV is expected to consume more fuel for tests on which the average wheel power request is high. Referring to Figure 8 it is expected that the fuel cell system will operate with a poor mean cycle efficiency for US06, RDE, WLTC, and BAB130 cycles which are the ones featuring highest mean wheel power requests (Figure 17). On average the Hyundai Nexo roughly consumes 0.98 kgH2/100 km on a typical type of use (average over RDE and WLTC). A 3% difference is reported between measured and approval value (=0.95 kgH2/100 km) of fuel consumption on WLTC. Notably, when lab temperature was set at 10°C a fuel consumption of 1.11 kgH2/100 km was observed on WLTC corresponding to a 21% increase as compared to the value obtained with compliant lab temperature conditions (23°C) (Figure 12).

Fuel cell performances and dynamic capabilities. BAB130 was run to assess the power dynamic capabilities of the fuel cell system as well as to reach a maximum transient system power. The fuel cell achieved a power ramp up to 90 kWe (at system level) in about 760 ms and held it for less than 1 s. On the same very dynamic load the battery power reached 39-kWe power output and was capable of absorbing a 35-kWe power input on regenerative breaking phase (Figure 13).

Fuel consumption over long idling period

The vehicle was put at rest with contact on to study its idling fuel consumption. During this period a periodical operating behavior of the fuel cell was observed. Every 8 min, approximately, the fuel cell system generated a 5-s power peak ranging from 2 to 4.5 kWe. Similarly every 45 min the fuel cell system generated, on average, a 10-kWe power step over a 100-s time period to sustain battery SOC. The smallest and more frequent power peaks are assumed to be meant to keep the fuel cell warm. Over this long idling period a fuel consumption of 12.4 g/h was reported (averaged over a time window upon which SOC variation was zero, Figure 14).

Fuel cell system thermal short analysis

Figure 15 depicts the evolution of the three temperature measurements on a WLTC cycle. For a reference usage such as the WLTC the thermostat opened up at 13 min whereas for the aggressive driving US06 cycle the thermostat opened up on average at 1 min and 30 s. When thermal steady-state was reached T_{cp} ranged between 55°C and 58°C.

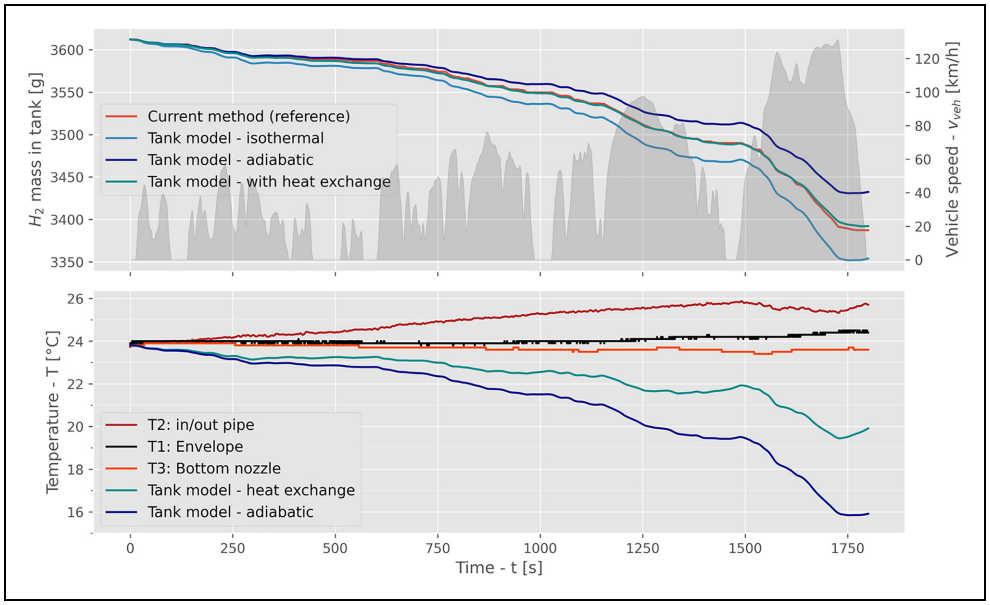

Figure 12. Evolution of hydrogen mass in tank calculated with the current method and compared to the results obtained solving the tank model during a WLTC cycle (top). Evolution of calculated hydrogen temperature throughout the cycle and tank temperature measurements (bottom).

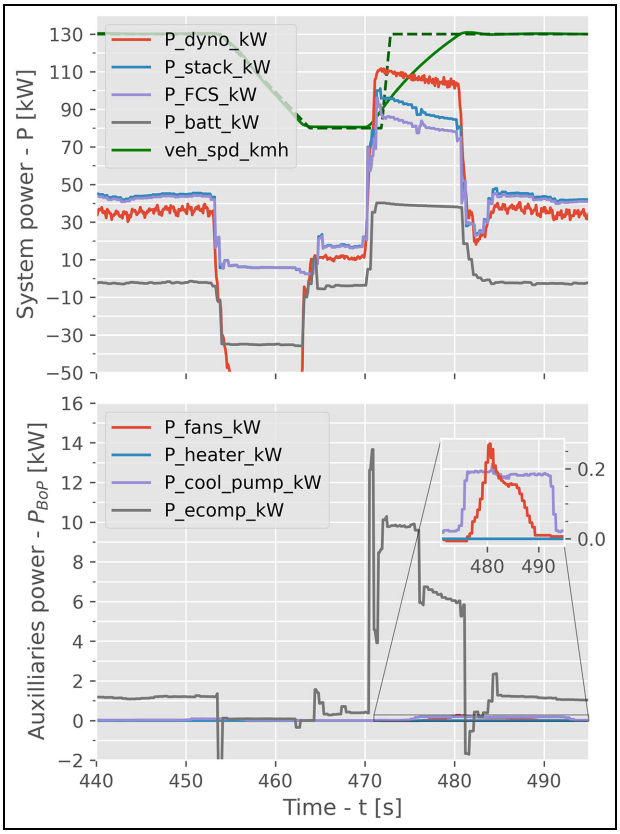

Figure 13. Acceleration from 90 km/h to 130 km/h on the ADAC highway BAB130 cycle. Dotted green line is the vehicle speed setpoint. A zoom in is applied to fans and cooling pump power consumption traces.

Figure 16 shows the evolution of the fuel cell efficiency with respect to cooling pump temperature which was considered as the best approximation of actual fuel cell coolant temperature. For cooling pump temperatures ranging from 10°C to 40°C the fuel cell stack efficiency was higher than during warm fuel cell operation (i.e. thermal steady-state operation). Conversely, the efficiency at system level followed the opposite trend. This is because the air compressor is operated at higher pressure ratio boosting the stack efficiency (cathode air pressure effect on oxygen oxidation reaction). This translates into an additional power expense for the system and then reduces the fuel cell efficiency at system level (see bottom left in Figure 16).

Vehicle efficiency and fuel cell system energy balance analysis

Integrating the BoP components power consumption allows for drawing an exhaustive energy balance of the fuel cell system on operated driving cycles. Additionally the fuel consumption and the dynamometer wheel power measurements are necessary variables to calculate the vehicle total efficiency defined as follows:

$$\eta_{veh} = \frac{E_{wheel}|_{P_{wheel}>0}}{E_{LHV_{H_2}}} \tag{13}$$

With $E_{wheel}|_{P_{wheel}>0}$ [J] being the positive mechanical wheel energy expense measured at the dynamometer and $E_{LHV_{H_2}}$ [J] the hydrogen fuel energy expense measured thanks to the fuel cell current method throughout a specific driving cycle.

Vehicle efficiency ranges from 57% to 64% depending mostly on the cycle-averaged wheel power request (even reaching 55% for unrealistic highway driving behavior on BAB130). It comes down to 50% on the WLTC @10°C (with HVAC turned on). Furthermore

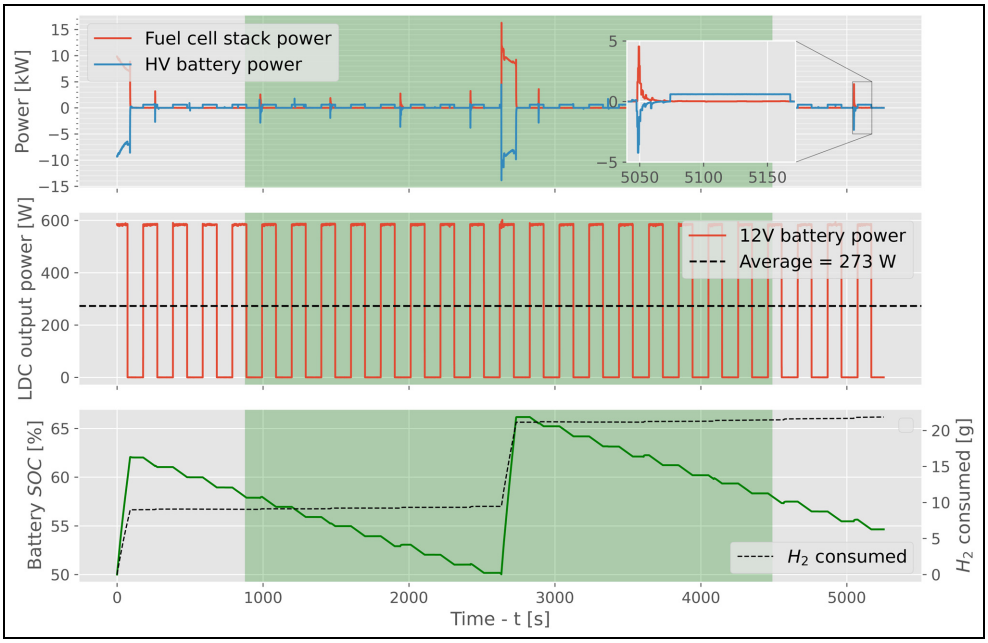

Figure 14. Long idling measurements. An iso-SOC time window was considered to determine idling fuel consumption (green-shaded background).

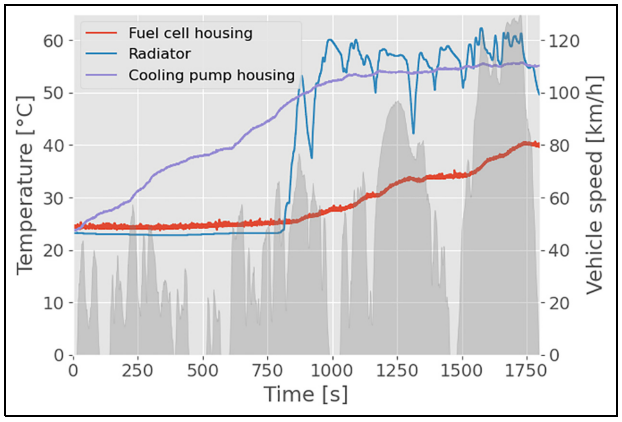

Figure 15. Temperature measurements on a WLTC.

it is worth to notice that the eCompressor accounts for the highest energy consuming component alongside with the 12-V accessories load (~280 W on all the cycles). Indeed, on average, the first one is consuming 2.5%–3% of the electrical energy generated by the fuel cell whereas the 12-V load is ranging from 2% to 6% of this same amount (Figures 17 and 18).

Conclusion

This paper has investigated the fuel cell powertrain behavior of the Hyundai Nexo on various mission profiles and characterized its global fuel cell system and vehicle efficiencies. Both the fuel cell current and the pressure methods yielded coherent results on fuel consumption evaluation, although discrepancies was found to reach up to 16% on FTP-75 cycles.

A hydrogen fuel consumption ranging from 0.67 kg/100 km for urban-type driving conditions to 1.24 kg/100 for very dynamic cycles was reported. Even when operating at reasonably low temperature, the FCEV revealed to consume significantly more fuel than in standard temperature conditions. Indeed, this study highlighted a 20% fuel consumption increase between the 10°C WLTC and the 23°C one. The reasons for this over-consumption are multiple: temperature effect on fuel cell stack efficiency, HVAC heater consumption, specific fuel cell heating strategy and temperature impact on battery ohmic resistance. More importantly, the vehicle fuel cell efficiency curve was derived on a dedicated power-step cycle. Accordingly, a maximum efficiency of 66.8% at fuel cell system level was experimentally witnessed. Yet, bearing in mind that the hydrogen purges were not accounted for, lower efficiency values are likely to arise with a hydrogen-flow measuring method.

As a consequence of uncertainties on initial tank temperature estimation and tank model hypotheses, the pressure method yielded different fuel consumption results as compared to the reference method (i.e. based on fuel cell current). Discrepancies between both methods were about 5% on average. This emphasizes the need for a hydrogen temperature sensor inside the tank to boost pressure method accuracy.

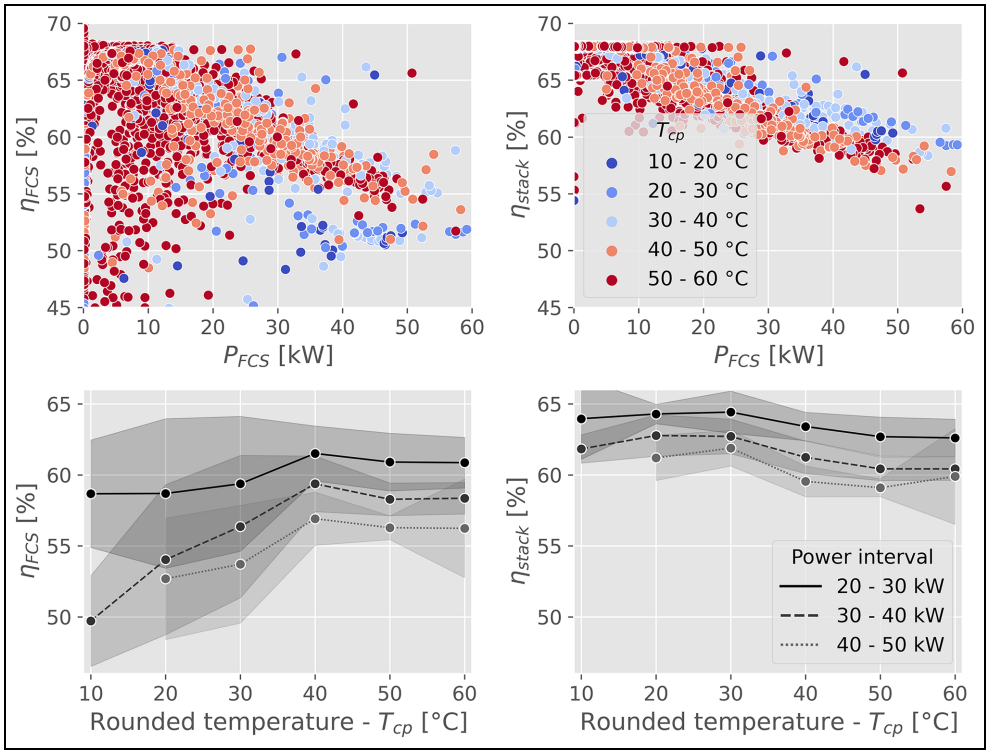

Figure 16. Temperature impact on fuel cell efficiency at both stack and system levels. Temperature measurements are rounded to the nearest 10. Shaded areas represent measurements standard deviations.

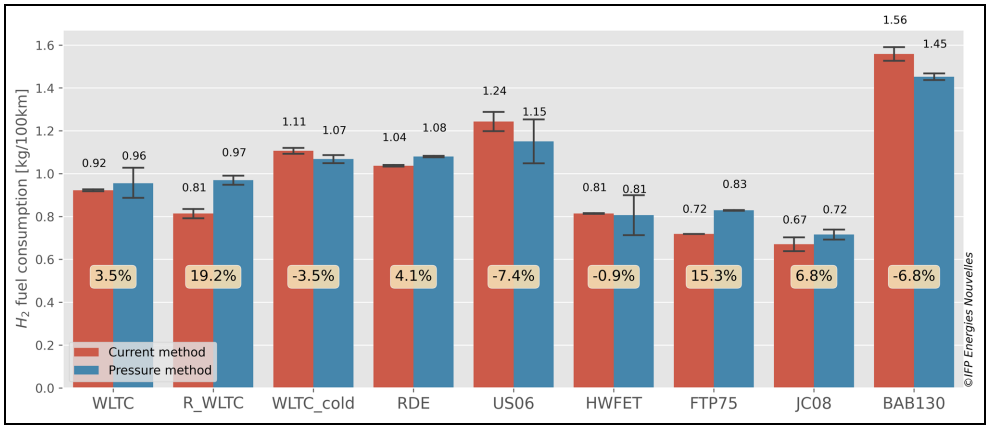

Figure 17. Comparison between fuel consumption measurement methods over the test campaign. The discrepancies between both methods are roughly 5% on average. The pressure method results turned out to be strongly driven by initial tank temperature estimation. This estimation was easy for cold start test before which the tanks rested a full night at ambient temperature. Conversely, for hot start tests, an error of 1°C on initial tank temperature (as a result of the tank model inherent uncertainties over the previous operated test) could induce up to a 5% fuel consumption difference.

Leveraging the fuel cell current-based method to determine hydrogen fuel power, energy balances were drawn at fuel cell stack, BoP and battery levels. Vehicle efficiency revealed to lie in a range spanning from 50% on WLTC@10°C to 64% for urban-type driving cycles (e.g. FTP-75 and JC08). Finally, this paper reported the significant contribution of both the electric air compressor and the 12-Volt accessories load in the fuel cell parasitic BoP energy consumption.

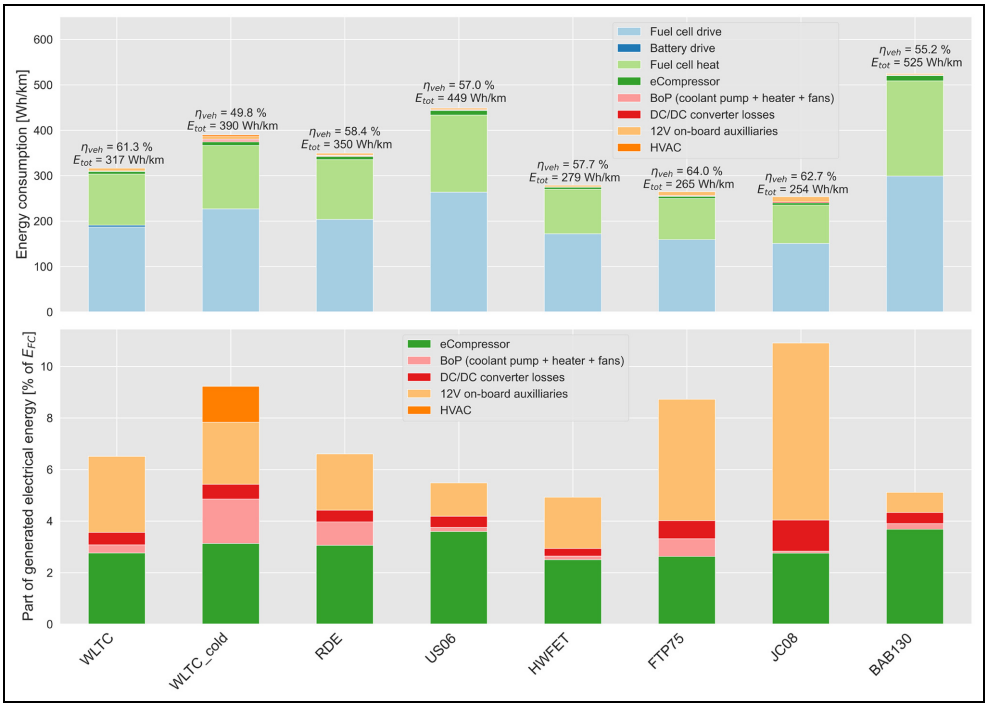

Figure 18. Vehicle energy balance on various driving cycles (top) and details on BoP and accessories energy consumption expressed as part of total generated fuel cell electrical energy (bottom).

Acknowledgement

The authors would like to thank all the colleagues who contributed to this work with a particular gratitude for those who worked on vehicle instrumentation and who conducted the tests on the dyno: P. Pauvert, X. Dunand, V. Brocchetto, O. Pajot, T. Lepage, S. Sarabi, P. Degeilh, A. Battiston.

Declaration of conflicting interests

The author(s) declared no potential conflicts of interest with respect to the research, authorship, and/or publication of this article.

Funding

The author(s) disclosed receipt of the following financial support for the research, authorship, and/or publication of this article: This work was supported and funded by IFP Energies Nouvelles.

ORCID iD

Jules Sery https://orcid.org/0000-0001-6307-2771

References

1. International Energy Agency (IEA). *Energy technology perspectives*, https://www.oecd ilibrary.org/content/publication/d07136f0en (2020).
2. International Energy Angency (IEA). *Global EV Outlook*, https://www.iea.org/reports/global-ev-outlook-2020 (2020).
3. Bodineau L and Sacher P. Rendement de la chaîne hydrogène - cas du power-to-H2-to-power, https://www.ademe.fr/sites/default/files/assets/documents/rendement-chaineh2fiche-technique-02-2020.pdf (2020).
4. BMW. *Hydrogen fuel cell cars: everything you need to know*. https://www.bmw.com/en/innovation/how-hydrogen-fuel-cell-cars-work.html (2019).
5. insideevscom. *Efficiency compared*, https://insideevs.com/news/332584/efficiencycompared-battery-electric-73-hydrogen-22ice-13 (2017).
6. Daud WR, Rosli RE, Majlan EH, Hamid SA, Mohamed R and Husaini T. Pem fuel cell system control: A review. *Renew Energy* 2017; 113: 620–638.
7. Hong BK and Kim SH. (invited) recent advances in fuel cell electric vehicle technologies of hyundai. *ECS Trans* 2018; 86(13): 3–11.
8. O'Hayre R, Suk-Won C, Whitney GC and Fritz BP. *Fuel Cell Fundamentals*. 3rd ed. New York: John Wiley Sons, 2016.
9. ECE/TRANS/180/Add15/Amend6. *United nations global technical regulation on worldwide harmonized light vehicles test procedures (WLTP)*. Global Technical Regulations from UNECE (United Nations), Standard, 2021.
10. ISO 23828. Fuel cell road vehicles – energy consumption measurement -Vehicles fueled with compressed hydrogen. International Organization for Standardization, Standard 2013.
11. SAE J2572. *Recommended practice for measuring fuel consumption and range of fuel cell and hybrid fuel cell vehicles fueled by compressed gaseous hydrogen*. SAE International, Standard, 2014.
12. Kuroda E and Yano M. An oxygen balance method: Fuel consumption measurement for fuel cell vehicles based on exhaust emissions with no vehicle modification. *Adv Automobile Eng* 2016; 5: 5.
13. Lohse-Busch HM, Duoba K, Stutenberg S, Iliev M and Kern. *Technology assessment of a fuel cell vehicle: 2017*

Toyota Mirai (Technical report). Argonne National Laboratory, Lemont, IL, 2018.
14. Lohse-Busch H, Stutenberg K, Duoba M, et al. Automotive fuel cell stack and system efficiency and fuel consumption based on vehicle testing on a chassis dynamometer at minus 18 °C to positive 35 °C temperatures. *Int J Hydrogen Energy* 2020; 45(1): 861–872.
15. Kurtz J, et al. *Fuel cell electric vehicle 2016 annual merit review*. NREL. U.S. Department of Energy (DOE), 2016.
16. GreenNCAP. *Hyundai Nexo vehicle testing*, https://www.greenncap.com/assessments/hyundai-nexo-2021-0069/ (2021).
17. Peng F, Ren L, Zhao Y and Li L. Hybrid dynamic modeling-based membrane hydration analysis for the commercial high-power integrated PEMFC systems considering water transport equivalent. *Energy Convers Manag* 2020; 205: 112385.
18. Bell IH, Wronski J, Quoilin S and Lemort V. Pure and pseudo-pure fluid thermophysical property evaluation and the open-source thermophysical property library coolprop. *Ind Eng Chem Res* 2014; 53(6): 2498–2508.
19. SAE J2799. *Hydrogen surface vehicle to station communications hardware and software*. SAE International, Standard, 2014.

Appendix

Acronyms

ADAC:	Allgemeiner Deutscher Automobil-Club
BHDC:	Battery High voltage DC/DC converter.
EoS:	Equation of State.
FBS:	Fully charged Battery Start.
FCEV:	Fuel Cell Electric Vehicle.
FCS:	Fuel Cell System.
FTP-75:	EPA Federal Test Procedure cycle.
HV:	High Voltage.
HWFET: EPA	Highway Fuel Economy Driving Schedule cycle.
HVAC:	Heating, Ventilation and Air Conditioning.
LHDC:	Low High voltage DC/DC converter.
LHV:	Lower Heating Value.
MEA:	Membrane Electrode Assembly.
NEDC:	New European Driving Cycle.
ODE:	Ordinary Differential Equation.
OOR:	Oxygen Oxidation Reaction.
RDE:	Real Drive Emission cycle.
SOC:	battery State-Of-Charge.
US06:	Supplemental Federal Test Procedure (SFTP) cycle.
WLTC:	Worldwide harmonized Light vehicles Test Cycle.